

# Contribution of fetal microchimeric cells to maternal wound healing in sickle cell ulcers

Mansour Alkobtawi,<sup>1\*</sup> Maria Sbeih,<sup>1\*</sup> Karim Souaid,<sup>2,3\*</sup> Qui Trung Ngô,<sup>1</sup> Dany Nassar,<sup>1,2,3</sup> Hugo Arbes,<sup>4</sup> Henri Guillet,<sup>5</sup> Anoosha Habibi,<sup>5</sup> Pablo Bartolucci,<sup>5</sup> Mathieu Castela,<sup>1,#</sup> Sélim Aractingi,<sup>1,2,3,#</sup> and Bénédicte Oulès<sup>1,2,3,#</sup>

<sup>1</sup>Cutaneous Biology Laboratory, Institut Cochin, INSERM U1016, UMR 8104, Paris; <sup>2</sup>Department of Dermatology, Hôpital Cochin, AP-HP Centre-Université Paris Cité, Paris; <sup>3</sup>University Paris Cité, Faculté de Médecine Paris Centre Santé, Paris; <sup>4</sup>Institut de Biologie Intégrative de la Cellule, Genomic Structure and Translation Laboratory, UMR\_9198, CEA, CNRS, Université Paris-Saclay, Orsay and <sup>5</sup>Department of Internal Medicine, Red Blood Cell Genetic Diseases Unit, Hôpital Mondor, AP-HP, Hôpitaux Universitaires Henri Mondor, Créteil, France

*\*MA, MS and KS contributed equally as co-first authors.*

*#MC, SA and BO contributed equally as co-senior authors.*

**Correspondence:** S. Aractingi  
[selim.aractingi@gmail.com](mailto:selim.aractingi@gmail.com)

**Received:** March 29, 2022.

**Accepted:** October 31, 2022.

**Early view:** November 10, 2022.

<https://doi.org/10.3324/haematol.2022.281140>

©2023 Ferrata Storti Foundation

Published under a CC BY-NC license



## **Supplementary methods**

### **Immunostaining**

Wounds were embedded in optimal cutting temperature (OCT) compound (Life Technologies) and stored at -80°. Five µm OCT sections were cut using a Thermo Cryostar Nx70 (Thermo Fisher Scientific) and fixed for 10 min in 4% paraformaldehyde. Sections were permeabilized and blocked for 1 h in freshly prepared PB buffer (0.5% skim milk powder, 0.25% gelatin from cold water fish skin, 0.5% Triton X-100, 20 mM HEPES, 0.9% NaCl, pH 7.2 (all reagents from Sigma-Aldrich)). Antibodies were diluted in PB buffer for 1 h at room temperature. PBS (Life Technologies) / 0.05% Tween-20 (Sigma-Aldrich) was used for washes and Prolong Gold Antifade Mountant (Thermo Fisher Scientific) for mounting. Immunofluorescence images were acquired using a Nikon Eclipse 90i fluorescent microscope (Nikon). Photographs of at least 3 different fields were taken, and labelled cells were counted by fluorescence densitometry using ImageJ software (NIH), and reported as percentage of total nuclei.

### **RNA extraction, quantitative RT-PCR and RNA sequencing**

Total RNA extraction, reverse transcription, and PCR were performed as previously described.<sup>17</sup> Gene expression levels were normalized against *Gapdh* housekeeping gene. All the primers were from Qiagen (QuantiTect).

RNA sequencing was performed on sorted eGFP<sup>+</sup> fetal cells from peripheral blood of wounded and unwounded post-partum wild-type mice at day 1 post-wounding, and on sorted eGFP<sup>+</sup> positive fetal cells from digested wounds of post-partum SAD mice at day 3 post-wounding. RNA Sequencing was also performed on digested wounds of virgin and post-partum SAD mice at day 3 post-wounding. RNA sequencing analyses were performed at the Genomic Platforms

of Institut du Cerveau (ICM, Paris, France) and Institut Cochin (Paris, France), with an Illumina Hi-Seq device (2 reads x 25 million fragments, paired-end 2 x 100 nt).

### **Cell Culture and flow cytometry**

Female mice mated with eGFP males were sacrificed 8 weeks after delivery. Bone marrow cells were obtained upon flushing posterior legs bones using 1 mL of PBS pH 7.4 (Life Technologies) with a 25G needle (Terumo). Cells were grown at a density of 100,000 cells per well in EGM-2 medium supplemented with 10% Fetal Veal Serum (Gibco) and 1% penicillin / streptomycin (Gibco). Colony size was assessed after 9 days of culture.

Colonies were dissociated to obtain a single-cell suspension. Antibodies used for cytometry were CD11b-PERCP-Cy5.5 (1:100; eBioscience), CD31-PE-Cy7 (1:100; eBioscience), CD34 APC (1:100; eBioscience), CD45 APC (1:100; eBioscience). Flow cytometry data were acquired using a BD LSRII (BD Pharmingen), and analyzed with FlowJo v8 software (BD Biosciences).

### **Computational analyses**

Analysis of RNA sequencing was performed using R version 3.6.1 (<https://www.r-project.org>). Raw data quality was checked using fastqc v0.11.9 (<https://www.bioinformatics.babraham.ac.uk/projects/fastqc/>). Reads were trimmed by cutadapt v3.1 (<https://cutadapt.readthedocs.io/en/stable/reference.html>) to remove adapters used for the sequencing. Alignment was performed on GRCm38.p6 mouse genome by hisat2 v2.2.1 (<http://daehwankimlab.github.io/hisat2/>). Formatting files and filtering high quality and uniquely mapped reads were done with samtools v1.11 (<https://www.htslib.org>). Assembly was done using the GRCm38.p6 genome annotations file ([http://www.ensembl.org/Mus\\_musculus/Info/Index](http://www.ensembl.org/Mus_musculus/Info/Index)). The read counts associated to each gene

were calculated by htseq v0.12.4 (<https://htseq.readthedocs.io/en/master/>). Differential expression analysis was done using DESeq2 v4.0.3 (<https://bioconductor.org/packages/release/bioc/html/DESeq2.html>) with an adjusted p-value threshold of 0.05. Data visualization, canonical pathways and upstream regulators analyses were performed using Ingenuity Pathway Analysis (IPA, Qiagen) with an adjusted p-value threshold of 0.05. Identification of putative cell types was performed using ARCHS4 (<https://maayanlab.cloud/archs4/index.html>).



## Supplementary Figure legends

### **Figure S1 - Skin wound healing is improved in pregnant mice.**

A. Representative images of wounds at days 0, 3, and 5, and planimetry of wound area at each time point relative to the original wound area.

B. Representative images and measurement of anti-K14 labelling of neo-epidermal tongues and wound gap at day 5.

C. Representative images and quantification of Ki67-positive cells in the wound bed at day 5.

D. Representative images of CD31-positive cells and quantification of vessel area in the wound bed at day 5.

Data information: Scale bars: 1000  $\mu\text{m}$  (B), 50  $\mu\text{m}$  (C-D). In (B-D), nuclei were counterstained with DAPI. In (A-D), four 6-mm excisional wounds were performed in virgin or pregnant mice (n=3 mice for each group). Data are presented as means with SD and individual values. Statistical analyses were performed with two-tailed t-tests with Welch's correction whenever required (A-B, D) or Mann-Whitney test (C). (\*) p-value < 0.05; (\*\*) p-value < 0.005; (\*\*\*\*) p-value < 0.00005.

### **Figure S2 - Wound vascular angiogenesis is improved in pregnant mice while infiltration by macrophages and neutrophils is not significantly changed.**

A. Quantitative RT-PCR analysis of *Vegfa*, *Vegfr1*, *Vegfr2*, *Vegfc*, and *Vegfr3* mRNA expression in the wounds at day 5 of virgin and pregnant mice as normalized to mRNA *Gapdh* level.

B. Representative images and quantification of F4/80-positive macrophages in the wound bed at day 5.

C. Representative images and quantification of GR1-positive neutrophils in the wound bed at day 5.

Data information: Scale bars: 50  $\mu\text{m}$  (B-C). In (B-C), nuclei were counterstained with DAPI. In (A-C), 4 6-mm excisional wounds were performed in virgin or pregnant mice (n=3 mice for each group). Data are presented as means with SD and individual values. Statistical analyses were performed with two-tailed t-tests with Welch's correction whenever required (A for Vegfa, Vegfr1 and Vegfr3, C) or Mann-Whitney test (A for Vegfc and Vegfr2, B). (ns) not significant; (\*) p-value < 0.05.

**Figure S3 – Fetal microchimeric cells are recruited to wounds in post-partum mice.**

A. Representative images and quantification of GFP-positive cells in the wound bed at day 3 in virgin and post-partum mice.

B. Representative images and quantification of GFP-positive cells in the wound bed at day 5 in virgin and post-partum SAD mice.

Data information: Scale bars: 100  $\mu\text{m}$ . Nuclei were counterstained with DAPI. In (A), two 6-mm excisional wounds were performed in virgin or pregnant mice (n=2 mice for each group). In (B), one 8-mm excisional wounds were performed in virgin (n=4 mice) or post-partum SAD mice (n=5 mice). Data are presented as means with SD and individual values. Statistical analyses were performed with Mann-Whitney test. (\*\*) p-value < 0.005; (\*\*\*) p-value < 0.0005.

**Figure S4 - Fetal microchimeric cells display progenitors features and express immune markers.**

A. Brightfield and fluorescence microscopy representative images of marrow-derived eGFP-positive FMC and their unlabeled adult counterparts seeded at low density and grown in EGM-

2 media. Colony size was assessed after 9 days of culture. An eGFP-negative colony is highlighted by the white dashed circle. Scale bars: 50  $\mu$ m. Data are presented as means  $\pm$  standard errors of the mean. Statistical analyses were performed with two-tailed t-test. (\*) p-value < 0.05.

B. eGFP-negative and eGFP-positive marrow-derived cells were isolated by FACS sorting after 9 days of culture as in (A). Representative FACS results for CD45, CD34, CD11b and CD31 stainings versus Forward Scatter (FSC) intensity and quantifications as percentages of total events are presented.

**Figure S5 - Ever parous SCD patients display less severe leg ulcers than nulliparous SCD patients.**

A-H. Several parameters reflecting ulcers severity were quantified in nulliparous and ever parous SCD patients: hospitalization (A), sick leave (B), infection (C), depression (D), morphine use for leg ulcers (E), skin graft (F), bosentan or ilomedin treatment (G), and red blood cell exchange transfusion to treat leg ulcers (H).

Data information: Nineteen SCD patients with leg ulcers were included in the nulliparous group and 60 in the ever parous group. Data are presented as frequency over the total number of recorded events. Statistical analyses were performed with Fisher's exact test. (ns) not significant; (\*) p-value < 0.05.

**Table S1: TPM-normalized quantification of RNA abundance in RNAseq data of sorted eGFP+ fetal cells from peripheral blood obtained from unwounded post-partum mice.**

**Table S2: Differential expression analysis using DESeq2 of RNAseq data comparing sorted eGFP+ fetal cells from peripheral blood obtained from wounded and unwounded post-partum mice at day 1 post-wound.**

**Table S3: TPM-normalized quantification of RNA abundance in sorted eGFP+ fetal cells from skin wounds obtained from wounded post-partum mice at day 3 post-wound.**

**Table S4: Differential expression analysis using DESeq2 of RNAseq data comparing digested total wounds obtained from virgin and post-partum SAD mice at day 3 post-wounding.**

**Figure S1**

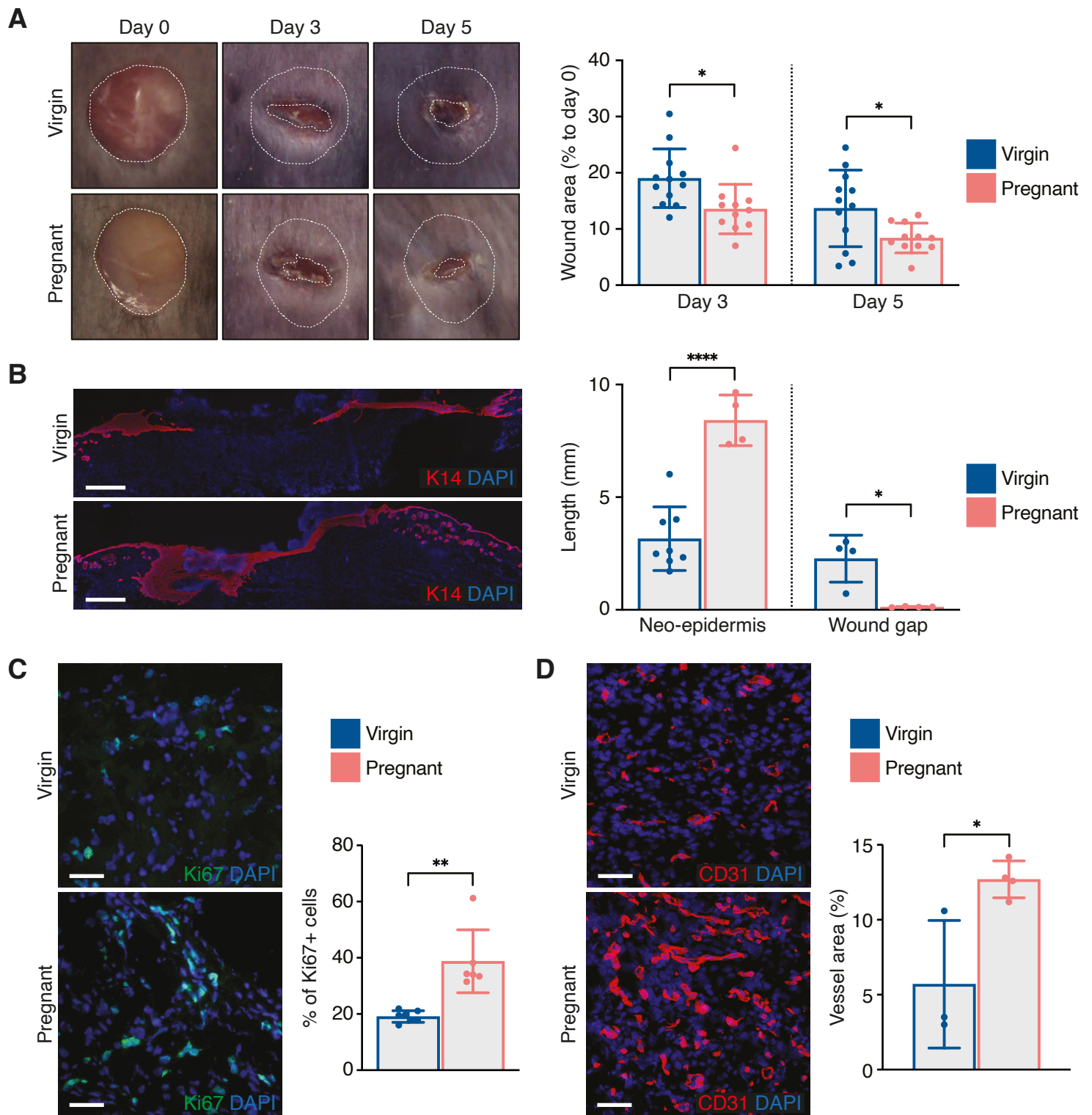
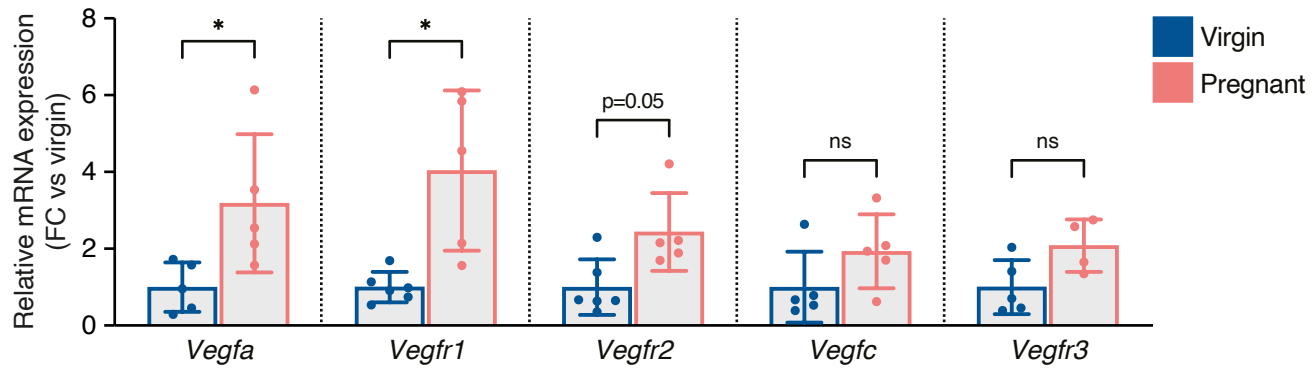
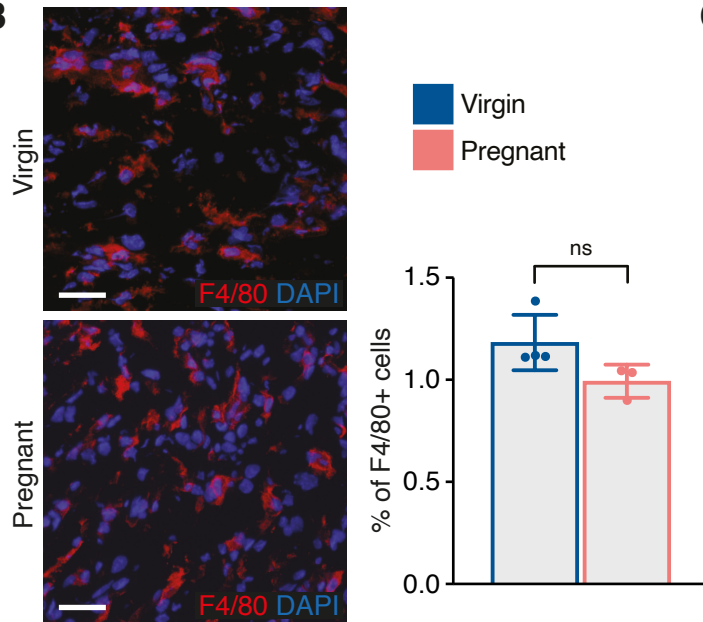


**Figure S2**

**A**



**B**



**C**

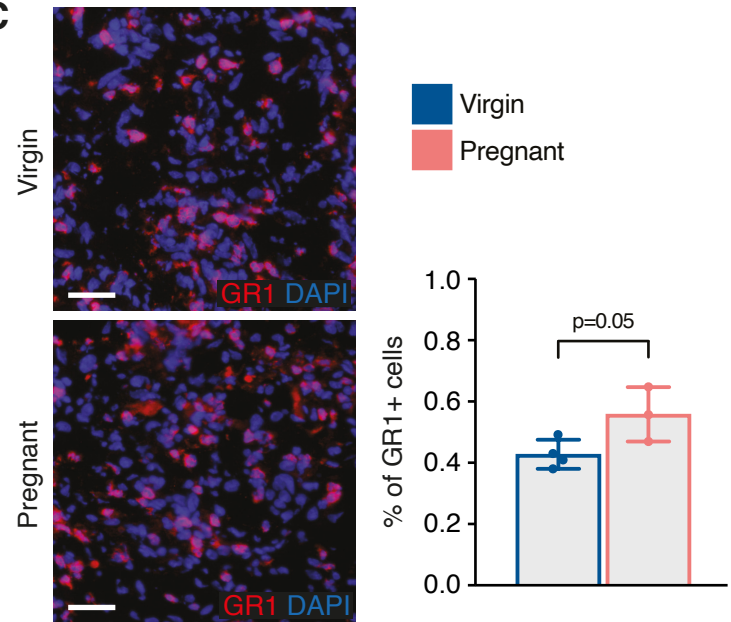


**Figure S3**

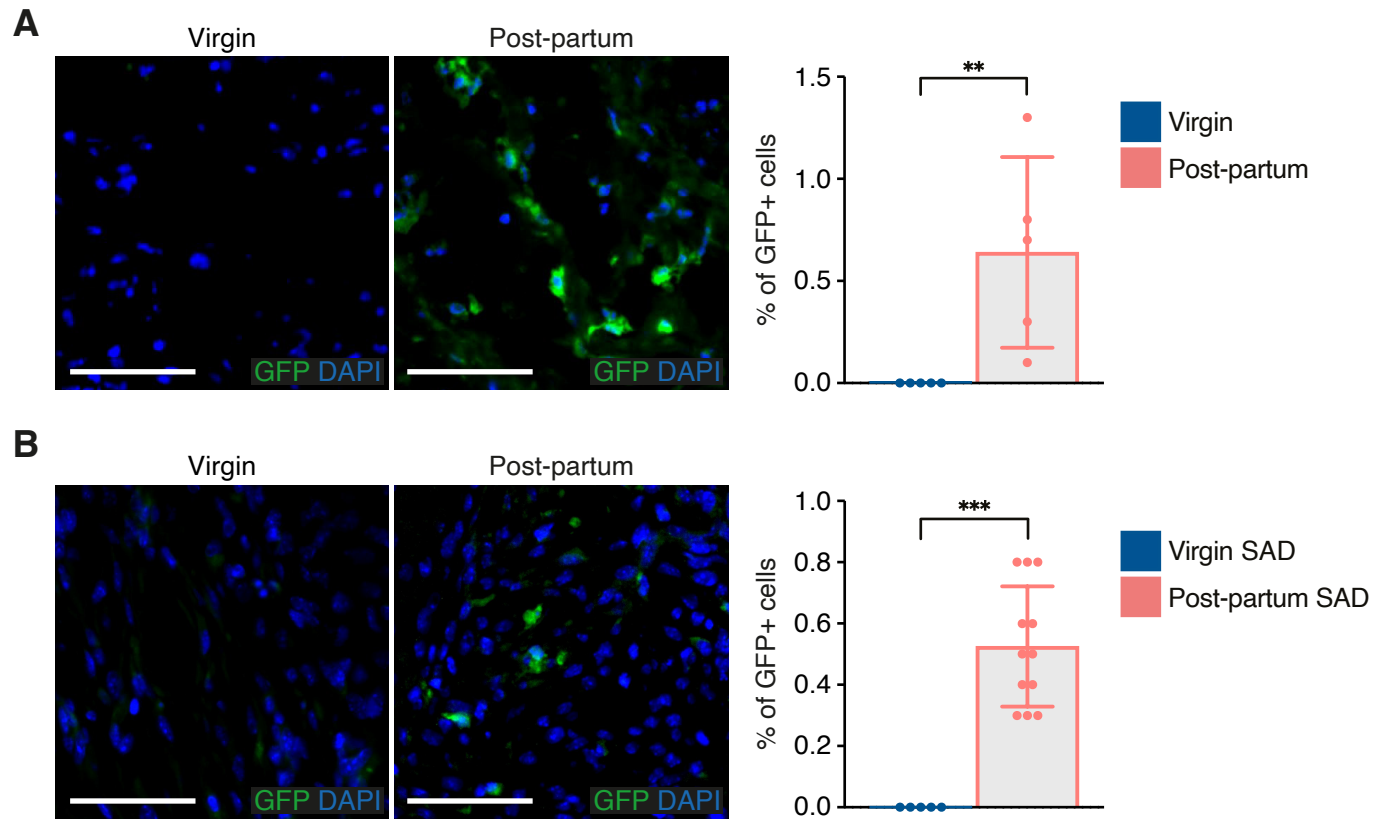
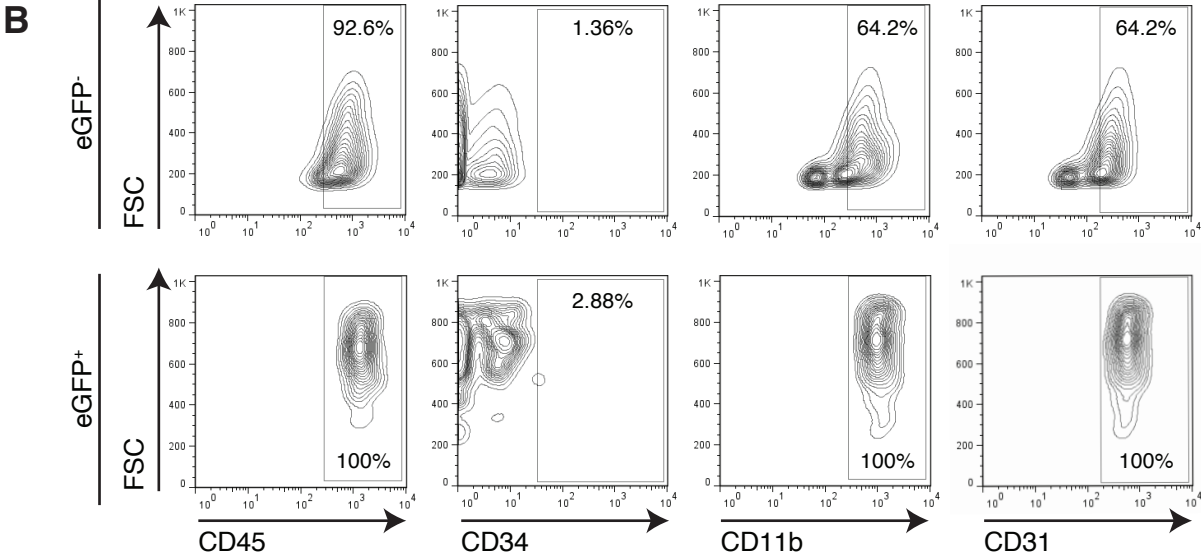
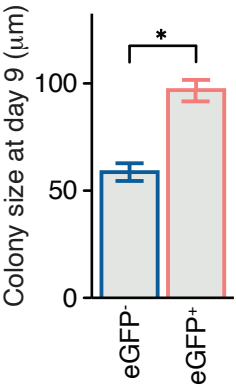
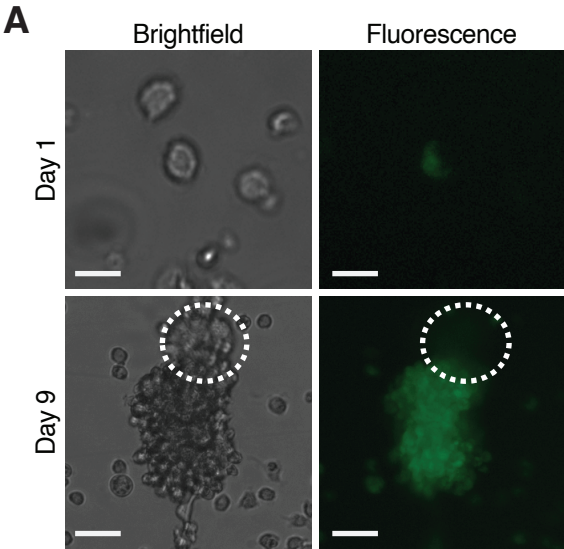


Figure S4





**Figure S5**

